Mon. Not. R. astr. Soc. (1984) **208**, 347–364

The Fe^{9+} region in active galactic nuclei

M. V. Penston, R. A. E. Fosbury and A. Boksenberg
Royal Greenwich Observatory, Herstmonceux Castle, Hailsham, Sussex BN27 1RP

M. J. Ward *Institute of Astronomy, Madingley Road, Cambridge CB3 0HA*

A. S. Wilson *Astronomy Program, University of Maryland, College Park, Maryland 20742, USA*

Received 1983 September 30; in original form 1983 June 8

Summary. Spectroscopic data at resolutions of 1 Å or better, including the [Fe X] λ 6374 Å line, are presented for 29 Seyfert and related galaxies. [Fe X] λ 6374 has certainly or probably been detected in 12 galaxies. The strength of both this line and [Fe XI] λ 7892 is correlated with that of the [Fe VII] and [O III] lines, suggesting the Fe^{9+} and Fe^{10+} ions are photoionized. A possible relation between [Fe X] and Hβ intensities is consistent with this view, although current photoionization models do not agree well with the observed relative intensities of the highly ionized iron lines. Alternatively, the line ratios may be reproduced by collisional ionization in a gas of temperature near 10^6 K, although a range of temperatures is needed. The probable variability of [Fe X] λ 6374 in NGC 4151 and the apparent absence of collisional de-excitation limit the radius of the Fe^{9+} zone to between 1×10^{-4} and 0.5 pc and its density to between 4×10^4 and 6×10^{11} cm^{-3}. The [Fe X] and [Fe XI] lines are blueshifted with respect to the systemic velocity of the galaxy, typically by $\simeq 120$ km s^{-1}, and are also broader than lines from lower ionization species. We ascribe these effects to a combination of higher outflow/inflow velocities closer to the central source and obscuration.

1 Introduction

The first report of very highly ionized iron in a Seyfert galaxy was by O. C. Wilson in 1956 (see Oke & Sargent 1968). Oke & Sargent identified lines of [Fe X] at λ 6374 and [Fe XIV] at λ 5303 in the spectrum of NGC 4151, but Weedman (1971) showed later that the line near λ 5303 was more probably associated with λ 5309 of [Ca V]. In a recent paper, however, Osterbrock (1981) reports that the [Fe XIV] line may be present in the Seyfert galaxy IIIZw77. Gradually, confidence in [Fe X] as the correct identification of the feature near

Table 1. [Fe X] λ6374 fluxes in NGC 4151.

Epoch	[O I]★/Hβ (×100)	[Fe X]/Hβ (×100)	[Fe X]/[O I]★	Reference
<1967	18	2.0:	0.11:	Oke & Sargent (1968)
1970 May/June		0.6	0.06	Weedman (1971)
1973 January		<0.6	<0.06	Netzer (1974)
1974 April	18	<1.2	<0.07	Boksenberg *et al.* (1975)
~1975	12	1.1	0.09	Osterbrock & Koski (1976)
1977 April			0.04	This paper
1979 June	14	1.5	0.10	Schmidt & Miller (1980)

★ Actually ([O I] λ6300 + [S III] λ6312).
No corrections for reddening have been applied.

λ6374 has grown (Phillips & Osterbrock 1975; Cooke *et al.* 1976; Osterbrock 1977); none of the possible alternative Fe II lines seems plausible. In addition, Grandi (1978) has identified the infrared line of [Fe XI] at λ7892 in several Seyferts.

Oke & Sargent (1968) originally proposed that the high excitation lines were emitted by a hot, collisionally ionized gas with a temperature of order 10^6 K surrounding, and in pressure balance with, filaments or clouds emitting lines of lower ionization species. Nussbaumer & Osterbrock (1970) calculated the resulting [Fe X] λ6374-to-[Fe XIV] λ5303 ratios as a function of temperature. Alternatively (Osterbrock 1969; Grandi 1978), the Fe^{9+}, Fe^{10+} and Fe^{13+} species may be photoionized, as is generally accepted for all the less highly ionized species like Fe^{6+}. In this picture, the high ionization lines originate from the innermost parts of the narrow line region and the temperature of the Fe^{9+} and Fe^{10+} regions will be $T \sim 3 \times 10^4$ K (Grandi 1978).

In his study of the [Fe XI] line, Grandi (1978) found that the kinematics of the Fe^{10+} region are different from that of the lower ionization regions; [Fe XI] λ7892 is slightly blue-

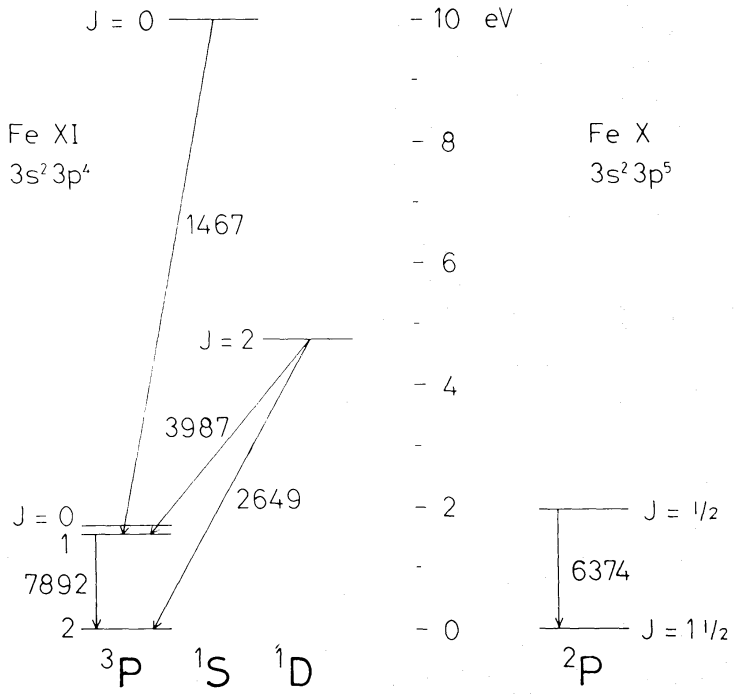

Figure 1. Partial Grotrian diagrams of Fe XI and Fe X showing the lines discussed in the paper.

shifted and, in two cases, broader than the other forbidden lines. The same results for [Fe x] λ 6374 were clearly demonstrated in NGC 3783 by Ward (1978), Wilson (1979) and Pelat, Alloin & Fosbury (1981). In fact, Wilson (1979) and Pelat, Alloin & Fosbury (1981) noted correlations in NGC 3783 between line width and ionization potential necessary to create the species, or alternatively between line width and transition probability. They suggested that the Fe^{9+} and Fe^{10+} regions are intermediate (in spatial scale, density and velocity spread) between the familiar broad and narrow line regions, a picture also favoured by Osterbrock (1981) for IIIZw77.

In view of the small spatial scale (≈ pc) of the Fe^{9+} region suggested by the photoionization models and by the kinematic data discussed above, possible variability of the [Fe x] λ 6374 line is of great interest. Netzer (1974) was the first to claim such variability in NGC 4151 and the relevant data are collected in Table 1. The case for variability on a timescale of three years or less is quite strong. Variability, within one year, has also been claimed for the [Fe x] line of 3C 390.3 by Barr *et al.* (1980) but confirmation of this result would be a prudent step. This probable variability underlines the importance of the Fe^{9+} region as a compact region close to the centre of activity in the galactic nuclei.

As a guide to the reader, for the later discussion, partial Grotrian diagrams of Fe^{9+} and Fe^{10+} are given in Fig. 1.

2 Data description and reduction

Data were taken using two different telescope–spectrograph combinations. During 1976 December, the 3.9-m Anglo-Australian telescope was used with the 25-cm camera of the Royal Greenwich Observatory spectrograph, giving a dispersion of 23 Å mm^{-1}. During 1977 July, the same telescope and spectrograph, but with the grating blaze to collimator, were used so that the dispersion was only 33 Å mm^{-1}. To cover some northern objects, the 5-m Hale telescope on Palomar Mountain was employed in 1977 April at the coudé focus to give a dispersion of 9 Å mm^{-1}. In all cases, an Image Photon Counting System (IPCS) was used and the resolution is 1 Å or better. More details of the observations are given in Table 2, the journal of observations. The targets observed were chosen to include Seyfert galaxies of both Types 1 and 2, galaxies known and not known (at the time) to be X-ray sources, so that the incidence and other properties of the [Fe x] line could be related to these parameters. It was anticipated, for example, that a continuum strong enough to be responsible for photoionizing Fe^{8+} might extend into the X-ray region. Sample data of objects with strong [Fe x] appear in Fig. 2.

It is unfortunate that the λ 6374 [Fe x] line always lies in the wing of the λ 6363 line of [O I] which is usually rather stronger. In order to study the [Fe x] line alone, however, it is possible to use the fact that the λ 6300 line of [O I] shares the same upper level as λ 6363 with a branching ratio of 3 : 1 in favour of the shorter wavelength line. By shifting the spectrum, so that λ 6300 moves to the position of λ 6363, and subtracting one third of the shifted line from the [O I] + [Fe x] blend, we have obtained the profile of [Fe x] λ 6374 free from this contamination. Any other spectral features will, of course, confuse this process and it is particularly inconvenient that [S III] λ 6312 – the high density line analogous to [O III] λ 4363 – is then shifted almost exactly onto the [Fe x] line. In fact, however, the [S III] line is sufficiently weak (especially after its intensity has been multiplied by 1/3) that this effect is unimportant with regard to the detection of [Fe x] λ 6374, although it may result in a slight systematic underestimate of the [Fe x] λ 6374 fluxes. A normal galaxy, NGC 720, subjected to this procedure also showed no spurious [Fe x] feature, suggesting there is also no problem from stellar absorption lines.

Table 2. Journal of observations.

Object	Date	Tel (in)	Disp (Å mm^{-1})	Time (s)
NGC 1052	1976 Dec 13	150	23	1000
NGC 3783	Dec 13	150	23	2000
NGC 3081	Dec 13	150	23	1000
Pictor A	Dec 14	150	23	2000
NGC 4507	Dec 20	150	23	1000
Mk 618	1977 Jan 4	150	45	4000
NGC 3516	Apr 3	200	9	2000
NGC 4151	Apr 3	200	9	4000
MCG 8-11-11	Apr 4	200	9	4000
Mk 79	Apr 4	200	9	2000
NGC 4051	Apr 4	200	9	4000
NGC 4151	Apr 4	200	9	2900
NGC 4507	July 19	150	33	4000
NGC 5506	July 19	150	33	4000
IC 4329A	July 19	150	33	4000
Mk 509	July 19	150	33	4000
NGC 7582	July 19	150	33	4000
NGC 7469	July 19	150	33	4000
Tol 0109 – 383	July 19	150	33	4000
NGC 1068	July 19	150	33	2000
3C120	July 19	150	33	3000
3C327	July 20	150	33	6000
NGC 6814	July 20	150	33	4000
IC 5063	July 20	150	33	6000
Mk 335	July 20	150	33	4000
ESO 290 – G01	July 20	150	33	2000
Ak 120	July 20	150	33	2000
NGC 5548	July 22	150	33	4000
ESO 141 – G55	July 22	150	33	4000
IZwl	July 29	150	33	2000
ESO 113 – IG45	July 29	150	33	1000
MCG-2-58-22	July 30	150	33	4000
ESO 113 – IG45	July 30	150	33	4000
NGC 720	July 30	150	33	2000

A total of 29 Seyfert or otherwise active galaxies plus ESO 290 – G01 was observed. This last galaxy was included because of reported [Fe X] λ 6374 emission (West *et al.* 1978); however, our spectra do not show the line to be present. We have certainly or probably detected [Fe X] λ 6374 emission in 12 of the programme galaxies (Tables 3 and 4).

3 Redshifts and line widths

The most reliable estimator of the systemic redshift of Seyfert galaxies is probably the 21-cm emission line of neutral hydrogen. Unfortunately, good H I profiles are available for only a small number of our programme galaxies (Heckman, Balick & Sullivan 1978; Mirabel & Wilson 1984). Despite this limitation, a comparison of the heliocentric redshifts derived from the present measurements of [O I] λ 6300 with the 2-cm H I data reveals excellent agreement:

Mean $[z([\mathrm{O\,I}]) - z(\mathrm{H\,I})] = 0 \pm 42\ \mathrm{km\,s^{-1}}$ (8 galaxies).

In this equation and the following ones, the error represents the standard deviation of the

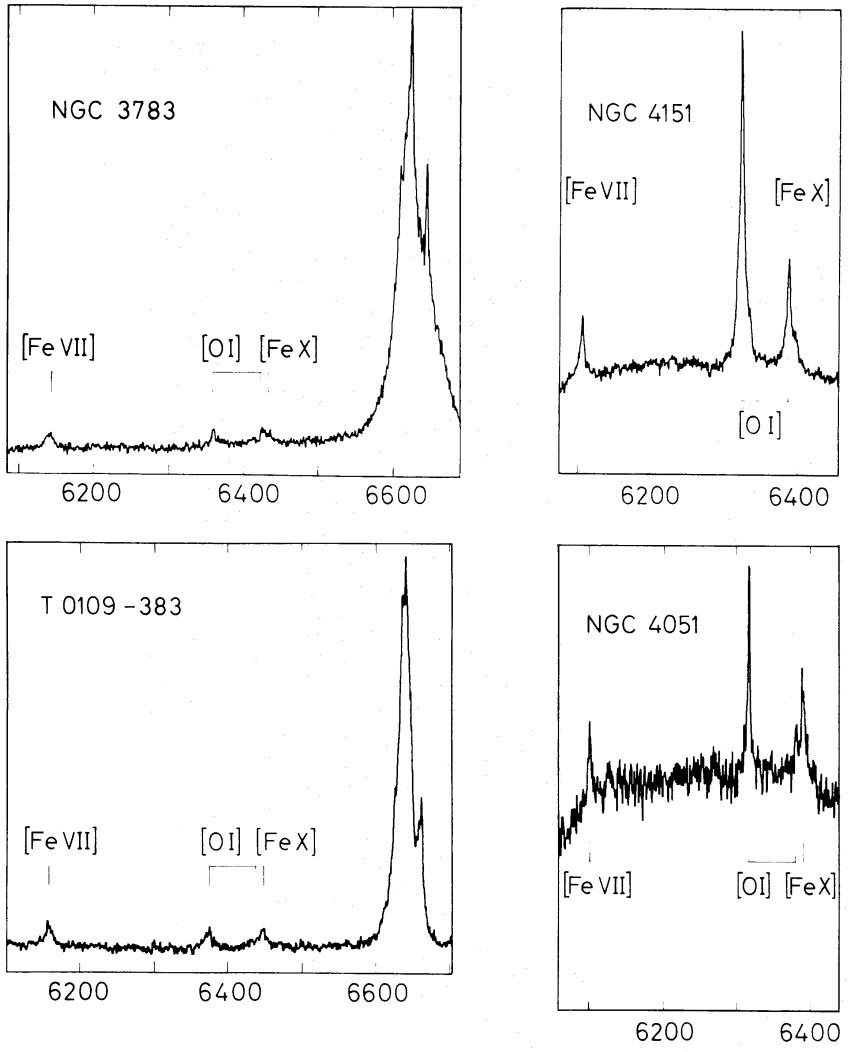

Figure 2. Spectra of four Seyfert galaxies with strong emission from [Fe X] λ6374.

mean. Similarly, the mean redshift of lines of low ionization species in our spectra (Hα, [N II], [S II] and [O I]*) agrees well with the H I measurements:

Mean $[z(\text{Low ionization}) - z(\text{H I})] = -10 \pm 40\ \text{km s}^{-1}$ (8 galaxies).

In the absence of 21 cm velocities for much of the sample, we may then use either [O I] λ6300 or the low ionization lines for the systemic redshift. On the other hand, the redshift of [O III] λ5007 tends to be lower than systemic (Heckman *et al.* 1981; Mirabel & Wilson 1984). In the present sample, only five galaxies have good H I profiles and [O III] velocities but the same result is apparent:

Mean $[z([\text{O III}]) - z(\text{H I})] = -88 \pm 21\ \text{km s}^{-1}$ (5 galaxies).

In view of these results, it is of interest to derive the velocity of the [Fe X] λ6374 line in the rest frame of the galaxy. Using the best estimate of the rest wavelength (6374.54 ±0.001 Å; Tyagun 1977), which is consistent with several other estimates of much lower quoted accuracy (e.g. Jefferies 1969; D. A. Allen, private communication), gives the velocities (and

* In some galaxies, not all of these lines were detected.

Table 3. Velocity and width of [Fe X] in rest frame of galaxy (as defined by [O I] λ 6300).

Object	Wavelength (Å)	Velocity (km s^{-1}) (assumes λ_0 = 6374.549)	FWHM (km s^{-1})
(a) Strong feature			
Tol 0109 – 383	6371.9	−125	532
NGC 3783	6369.9	−219	675
NGC 4051	6372.3	−106	770/190★
NGC 4151	6372.5	−96	380
Mean	6371.6 ± 0.6	−136 ± 28	
(b) Intermediate strength feature			
NGC 1068	6373.7	−40	820
NGC 3081	6369.4	−242	310:
NGC 4507	6377.1	+120	780
Ic 4329A	6372.9	−78	580:
NGC 5548	6371.7	−134	190:
NGC 7469	6368.5	−285	650:
Mean	6372.2 ± 1.3	−110 ± 60	
(c) Weak feature			
3C 120	6373.		410:
(Mk 618	6373.)		
(MCG8-11-11	6373.)		
(NGC 6814	6371.)		
Mk 509	6374.		1050:

★ Line may have two components of differing widths.

deconvolved widths) listed in Table 3. As may be seen, the [Fe x] velocities do, indeed, tend to be lower than systemic, with mean difference −120 ± 36 km s^{-1}; in only one galaxy (in addition to IIIZw77; Osterbrock 1981) is the line redshifted with respect to the galaxy. Grandi (1978) found an analogous blueshift for the [Fe XI] λ 7892 line, with mean offset from the other lines of −215 ± 65 km s^{-1} in seven galaxies. Three of his galaxies are in the present survey and the agreement between [Fe x] and [Fe XI] velocity shifts is gratifying (NGC 1068 [Fe x] −40 km s^{-1}, [Fe XI] −39 km s^{-1}; NGC 4051 [Fe x] −106 km s^{-1}, [Fe XI] −117 km s^{-1}; NGC 4151 [Fe x] −96 km s^{-1}, [Fe XI] −117 km s^{-1}). While the closeness of this agreement is probably fortuitous, it not only argues that the [Fe x] and [Fe XI] lines originate in similar regions of the nucleus, but also provides strong support for identification of the feature near λ 6374 with [Fe x].

The *widths* of lines from species of different levels of ionization are also of interest. Comparison of the [O I] λ 6300 width (present data) with that of [O III] λ 5007 (Heckman *et al.* 1981; Feldman *et al.* 1982) shows a significant difference. For the 11 galaxies in common to these surveys, the mean FWHM [O I] is 384 ± 67 km s^{-1} and the mean FWHM [O III] 505 ± 91 km s^{-1}. In nine of the 11 galaxies [O I] is narrower than [O III]. Sometimes (Pelat *et al.* 1981; Filippenko, private communication) it has been suggested that the line width may really be correlated with critical density rather than ionization potential. If this were so, [O I] would not be a typical low ionization species in this respect because of the high critical density of λ 6300 compared to [N II] and [S II] lines. The present data also show a trend for [Fe x] (mean FWHM 600 ± 250 km s^{-1}) to be broader than [O I]. A more complete discussion of the widths, redshifts and profiles of the low ionization species in Seyferts, based on a larger sample, is deferred to a later paper (Wilson *et al.*, in preparation).

Our results on the redshift and profile of the [Fe x] λ 6374 line confirm, therefore, the suggestion (Grandi 1978; Wilson 1979; Pelat *et al.* 1981) that the highly ionized species of iron originate from a region intermediate between the conventional broad and narrow line regions. They also show that a correlation between ionization state and line width, as found earlier for NGC 3783 (Wilson 1979; Pelat *et al.* 1981) and IIIZw77 (Osterbrock 1981), is a common feature of Seyfert galaxy nuclei. The kinematics of the [Fe x] zone are discussed further in Section 5.

4 Correlation of [Fe x] with other properties

Table 4 gives a number of properties of the galaxies in our programme. We list (from left to right) the name of the galaxy, the galactocentric redshift, the reddening $E(B-V)$, the equivalent width of [O I] λ 6300, the equivalent width of [Fe x] λ 6374, the luminosity of Hβ, the X-ray luminosity in the 2–10 keV band, the luminosity of the sum of [O III] λ 4949 and λ 5007, and the luminosities of [Fe VII] λ 6086, [Fe x] λ 6374 and [Fe XI] λ 7892. The reddening values are taken from a galactic cosecant law, $E(B-V) = 0.06 \operatorname{cosec} b$, except for a few cases (e.g. Tol 0109–383, NGC 1068, 3516, IC 4329A, NGC 5506 and 7582) where internal reddening has been demonstrated. The line luminosities have been calculated using the listed galactocentric redshifts and reddenings along with a Hubble constant of 50 km s^{-1} Mpc^{-1}. Calibration of the [Fe x] luminosities was achieved via published [O I] λ 6300 intensities and/or [O I] λ 6300/Hβ ratios along with Hβ intensities. In a few cases, as indicated, the [Fe x] measurements in Table 4 are strengthened by use of low dispersion (~120 Å mm^{-1}) data from the Anglo-Australian telescope/RGO spectrograph/IPCS combination.

The detection or non-detection of the [Fe x] line shows no preference between Seyfert type 1 and type 2 galaxies. In both cases, the present study finds emission in half the objects. Because of selection effects (the type 2 galaxies in our sample have a lower mean redshift than those of type 1) and the lack of any attempt to search for the line to a given flux level, we cannot derive the true distribution of [Fe x] luminosities in each type. However, in the present group of galaxies, the [Fe x] luminosity tends to be lower in Seyfert 2 type galaxies.

The ionization potential of Fe^{8+} is 235 eV. If photoionization is responsible for generation of the Fe^{9+} species, a correlation between [Fe x] λ 6374 and continuum luminosity near this wavelength might be anticipated. In view of the lack of direct measurements of the continuum at this wavelength, some test can be made by comparison of the [Fe x] intensities with soft X-ray fluxes and the hydrogen recombination lines. Comparison of [Fe x] and 2–10 kev flux densities (Fig. 3) shows a scatter diagram, suggesting no relation. The range of detected X-ray fluxes is, however, small and variability may be expected to wash out any correlation. A more conclusive test requires a larger sample and coordinated [Fe x] and X-ray measurements. The ultraviolet continua can be effectively sampled beyond 912 Å by observing the hydrogen recombination lines, although there is some question as to whether Lα or Hβ should do the job better – the well-known anomaly in the Lα/Hβ ratio suggesting a collisional origin for some fraction of Hβ. On the other hand, the variation in the Lα/Hβ ratio is only ± 0.3 rms in the logarithm and too small to mask a strong correlation with [Fe x] luminosity. A plot of [Fe x] flux against Lα flux for the rather few galaxies with measurements of both parameters yields a scatter diagram. In the [Fe x] versus Hβ flux plot (Fig. 4), however, a broad trend is apparent. A similar effect is seen if the luminosities are plotted, although part of the correlation in this plot may be attributed to the well-known selection effect resulting from observation of galaxies with a wide range in distance and a small range in apparent flux density.

Table 4. Emission line data.

Galaxy Seyfert type	cz (Galacto-centric) km s^{-1}	E_{B-V} mag	W*([OI]) Å	W*([FeX]) Å	log L(Hβ) erg s^{-1}	log L_x (2–10 keV) erg s^{-1}	log L([OIII]) (λ4959+λ5007) erg s^{-1}	log L([FeVII]) (λ6087) erg s^{-1}	log L([FeX]) (λ6374) erg s^{-1}	log L([FeXI]) (λ7892) erg s^{-1}
Mk 335 1	8052	0.08	0.4:	⩽0.6	42.62 (1)	⩽43.9	42.04 (2, 20)	40.91 (16, 19)	⩽40.28	40.87 (19)
IZw1 1	18422	0.07	⩽1.6	⩽1.6	42.90 (1)	⩽44.7	42.81		⩽41.37	
Tol 0109-383 2	3490	0.53	11.9	8.3	41.06 (21)	⩽42.8	41.81 (21)	40.34 (21)	40.26	
ESO 113-IG45 1 (F9)	13707	0.07	⩽1.0	3.6	43.36 (3)	44.4	42.66 (16)	41.42 (16)	41.41‡	
NGC 1052 2	1457	0.07	6.5	⩽0.6	40.52 (4)		41.00 (4)		⩽39.66	
NGC 1068 2	1064	0.63	23.0	1.2:	41.88 (2, 5)	⩽42.1	43.07 (2, 20)	41.28 (16, 19)	40.19: 40.32(5)	40.29 (16, 19)
3C 120 1	9935	0.12	8.7	2.7:	42.45 (1, 6, 15)	44.2	42.56 (2)	40.61: (18)	40.46:	
Mk 618 1	10559	0.10	⩽2.2	⩽2.2	42.54 (1)	43.7	42.11 (20)	40.95†	⩽40.82 40.70†	
Ak 120 1	9722	0.16	⩽1.3	⩽1.3	42.98 (16)	44.0	42.41 (16)		⩽40.94	
Pic A 1	10279	0.10	43.0	⩽4.4	41.38 (16)		41.93 (16)		⩽40.30	
MCG8-11-11 1	6248	0.32	17.1	⩽1.3	42.20 (20)	43.8	42.69 (20)	41.28 (16)	⩽40.66‡	
Mk 79 1	6727	0.12	3.4	⩽1.3	42.32 (1, 2, 8)	43.7	42.20 (2, 20)	40.42 (19)	⩽40.08	⩽39.28 (19)
NGC 3081 2	2290	0.13	5.0	1.0	40.51 (16)		41.84 (16)	40.22 (16)	39.30	⩽39.60 (16)
NGC 3516 1	2779	0.54	2.1:	⩽0.6	42.31 (1, 9)		42.15 (2, 20)	41.23 (19)	⩽40.48	⩽39.14 (19)
NGC 3783 1	2746	0.14	2.3	3.2	41.72 (2, 7, 14)	43.4	41.87 (2)	41.03 (16)	40.51	
NGC 4051	776	0.06	4.8	3.6	39.85	⩽41.5	40.17	38.62	38.93	38.44

NGC 4507 2	3368	0.14	14.0	2.2:	40.99 (16)	41.5	42.06 (16)	40.18 (16)	39.57:	
IC 4329A 1	4566	0.79	2.1	1.0	43.00 (11)	43.9	42.86 (11)	41.31 (11)	40.98	
NGC 5506 2	1811	0.60	62.0	≤1.9	41.30 (12)	43.0	42.30 (12)	40.00 (12)	≤39.56	
NGC 5548 1	5001	0.06	1.5	0.5:	41.99 (1, 7)	43.7	42.06 (2, 20)	40.89 (16, 19)	40.06:	39.55 (19)
3C 327 2	31244	0.06	7.2	≤2.2	41.34 (13)		42.72 (13)	41.06 (16)	≤40.82	
ESO 141-G55 1	11026	0.13	0.9	≤0.6	42.87 (3)	44.2	42.37 (16)	41.18: (16)	≤40.47	
NGC 6814 1	1745	0.21	1.4	≤0.6	40.80 (16)	42.8	40.65 (20)		≤39.42	
Mk 509 1	10544	0.12	1.4	1.0:	42.67 (1)	44.4	42.94 (20)	≤40.40 (16)	40.70:	
IC 5063 2	3370	0.09	15.1	≤1.0	40.80 (16)		41.90 (16)	39.64: (16)	≤39.56	≤39.91 (16)
NGC 7469 1	5084	0.08	3.1	1.8:	42.23 (1)	43.7	42.20 (2, 20)	40.49 (16, 19)	40.47:	≤40.08 (19)
MCG-2-58-22 1	14099	0.07	3.8:	≤0.6	43.28 (3)	44.8	42.81 (16)		≤40.71	
NGC 7582 2	1595	1.26	2.3	≤0.6	42.00 (3)	42.8	42.46 (16)		≤40.16	

★ The upper limits should be multiplied by $\sqrt{A/10}$ where A is the width of the line in Å.

× From reference 7, McHardy *et al.* (1981), Piccinotti *et al.* (1982), Mushotzky (private communication) or Kriss *et al.* (1980). The data in this last paper were converted to a luminosity in the 2–10 keV band assuming a spectral index $\alpha = 0.6$ and no absorption.

† Low dispersion observation.

‡ From V mag and equivalent width.

References

1. Weedman (1976).
2. Adams & Weedman (1975).
3. Ward *et al.* (1978).
4. Fosbury *et al.* (1978).
5. Koski (1978).
6. Shields (1974).
7. Elvis *et al.* (1978).
8. Neugebauer *et al.* (1976).
9. Boksenberg & Netzer (1977).
10. Boksenberg *et al.* (1975).
11. Wilson & Penston (1979).
12. Wilson *et al.* (1976).
13. Penston & Fosbury (1978).
14. Osmer, Smith & Weedman (1974).
15. Phillips & Osterbrock (1975).
16. This paper.
17. Anderson (1970).
18. Osterbrock (1977).
19. Grandi (1978).
20. Yee (1980).
21. Fosbury & Sansom (1983).

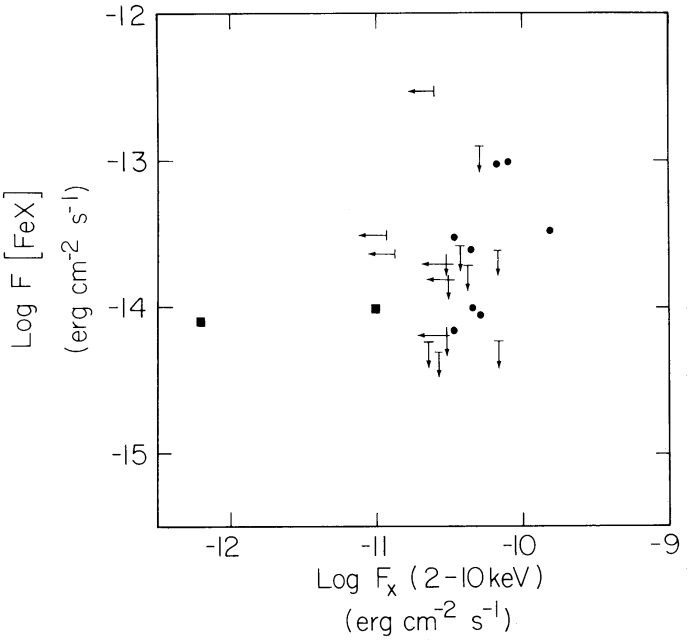

Figure 3. Plot of the flux density in the [Fe X] λ 6374 line against that in the 2–10 keV band. The X-ray data are taken from Elvis *et al.* (1978), Kriss, Canizares & Ricker (1980), McHardy *et al.* (1981), Piccinotti *et al.* (1982) and Mushotzky (private communication). The *Einstein* data (Kriss *et al.* 1980), represented by filled squares, were converted to 2–10 keV fluxes assuming a spectral index $\alpha = 0.6$ and no absorption.

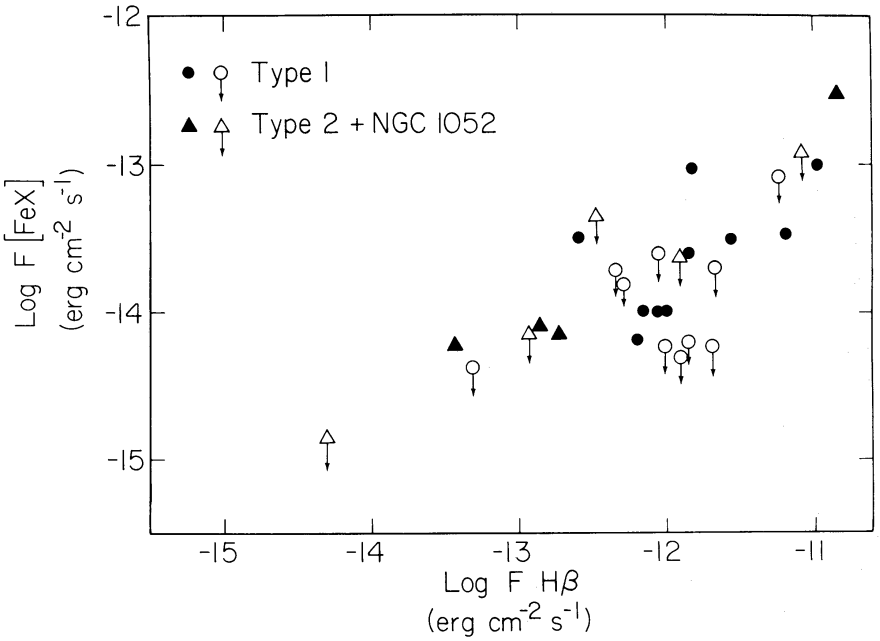

Figure 4. Plot of the flux density in the [Fe X] λ 6374 line against that in Hβ. Seyferts of type 1 and 2 are plotted separately.

The probable correlation with Hβ is consistent with a photoionization origin for the Fe^{9+} species. This conclusion is strengthened by correlations between [Fe X] and both [Fe VII] and [O III] intensities (Figs 5 and 6). A similar correlation between [Fe XI] and [Fe VII] was noted by Grandi (1978). Temperature estimates are available for the Fe^{6+} zone giving, for example, 2×10^4 K for IIZw77 (Osterbrock 1981), 3.5×10^4 K for Tol 0109 – 383 (Fosbury & Sansom 1983) and 1.1×10^4 K for NGC 4151 (Boksenberg *et al.* 1975). These temperatures

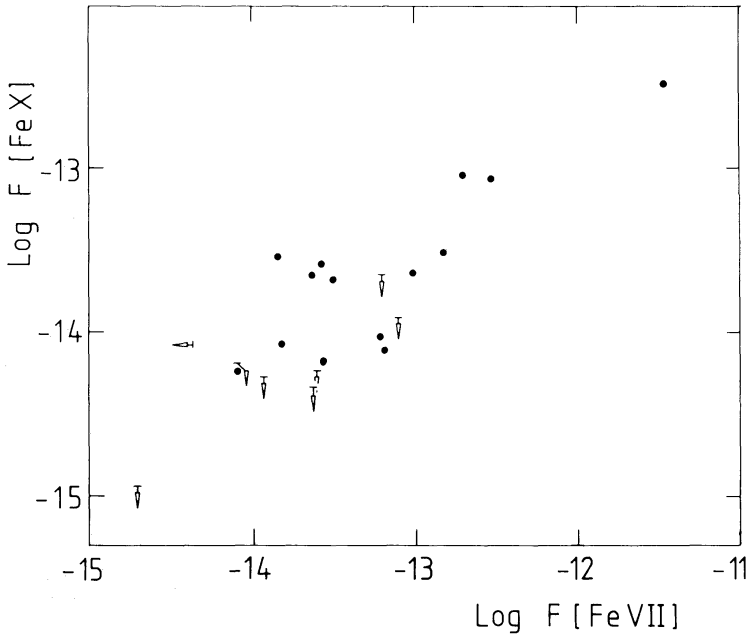

Figure 5. Plot of the flux density in the [Fe X] λ 6374 line against that in [Fe VII] λ 6087.

rule out collisional ionization for Fe^{6+} and strongly favour photoionization. The good correlations of [Fe X] and [Fe XI] with [Fe VII] then favour photoionization as the origin of these species too.

Unfortunately there are not enough objects in common between our survey and that of Grandi to investigate any possible connection between the [Fe X] and [Fe XI] fluxes. Although the line intensities are not measured at the same epochs, it is of interest to compute the intensity ratio $I(\lambda 6374)/I(\lambda 7892)$, which varies amongst the objects: 3.3 (NGC 5548), 3.1 (NGC 4051), 0.9 (NGC 1068) and 0.5 (NGC 4151). Two lower limits $\gtrsim 2.5$ (NGC 7469) and $\gtrsim 0.5$ (NGC 3081) fall in this range, as do Osterbrock's (1981) and Ward & Morris's (1984)* measurements of 2.0 in IIIZw77 and 1.5 in NGC 3783 respectively, but one upper limit extends it to $\lesssim 0.3$ (Mk 335). Omitting the limits, the mean of these measures gives a λ 6374/λ 7892 ratio of 1.9.

Two other lines of highly ionized iron are relevant to our discussion. The first is [Fe XIV] λ 5303, which is blended in Seyferts with the stronger line [Ca V] λ 5309. [Fe XIV] has been detected in IIIZw77 and NGC 3783, where respectively $I(\lambda 5303)/I(\lambda 6374) \sim 0.32$ (Osterbrock 1981) and ~ 0.5 (Ward & Morris 1984), but limits can be set for other objects. In the case of Tol 0109 – 383 (Fosbury & Sansom 1983), where the strong [Fe X] line should give a tight limit, the wavelength of the [Ca V] line was measured on two independent low-dispersion spectra giving rest wavelengths $\lambda_0 = 5309 \pm$ Å and 5306 ± 2 Å. This lack of displacement limits any contribution from [Fe XIV] to less than 0.3 of the whole feature and sets the limit $I(\lambda 5303)/I(\lambda 6374) \lesssim 0.15$ in this galaxy. The second line is λ 2649 of [Fe XI]. In NGC 4151, Penston *et al.* (1981) find a line close to this wavelength with reddening corrected luminosity $\simeq 7 \times 10^{39}$ erg s^{-1}, implying $I(\lambda 2649)/I(\lambda 7892) \sim 2$ if [Fe XI] is the correct identification. For Tol 0109 – 383, unpublished *IUE* data by Bergeron & Penston give an upper limit to the λ 2649 line flux of 1.6×10^{-14} erg cm^{-2} s^{-1} corresponding to a line

* Where we have used the data of Ward & Morris (1984) which became available at a late stage in the production of this paper, we have retained our value $E(B-V) = 0.14$ rather than their value $A_V = 0.8$) for compatibility with the rest of our paper.

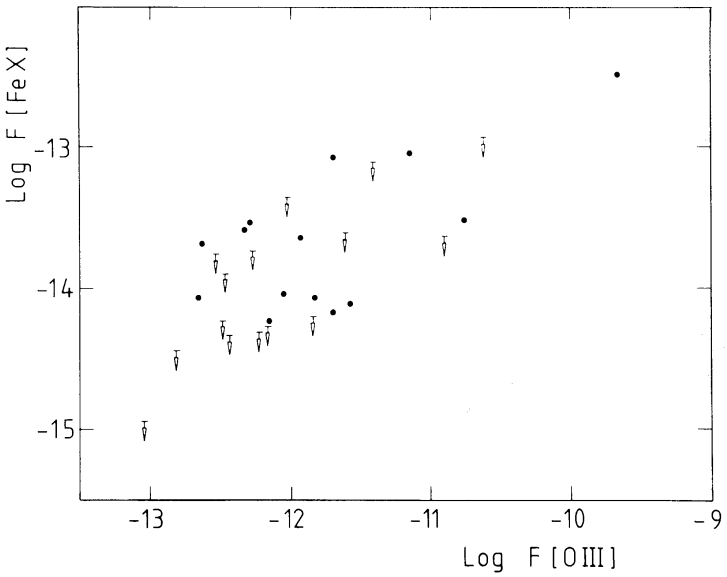

Figure 6. Plot of the flux density in the [Fe X] λ 6374 line against that in [O III] λ 4959 + λ 5007.

luminosity limit of 1.0×10^{40} erg s^{-1} if the absorption $A_V = 1.6$ mag. The data of Ward & Morris (1984) give $I(\lambda 2649)/I(\lambda 7892) < 2.3$ in NGC 3783. These line ratios, whose values are once again subject to uncertainty because of non-simultaneity of observation, are summarized in the 'observed' column of Table 5.

5 Discussion of the Fe^{9+} region

5.1 TEMPERATURE AND IONIZATION MECHANISM

The most direct way to distinguish between collisional and photionization mechanisms would be to measure the temperature of the emitting gas. The only true temperature diagnostic, which does not assume the ions co-exist or any other particular layering structure, is the [Fe XI] line ratio λ 2649/λ 7892. Unhappily, however, the variation in this ratio between $T = \infty$ and $T = 3 \times 10^4$ K is only a factor of ~ 2, its range being reduced somewhat below even the change indicated by the Boltzmann factor by the effects of cascades at higher temperatures (H. E. Mason, private communication). Thus, very accurate measurements are needed to use this ratio as a diagnostic. Such cannot be made for the ultraviolet line at present with the *IUE* satellite; the higher signal-to-noise data expected from the *Space Telescope* instrumentation may be able to distinguish temperatures characteristic of collisional ionization (~ 10^6 K) from those appropriate to photoionization (3×10^4 K).

In the absence of a clean discriminant between the two ionization modes, we are forced to compare the observed line ratios with model calculations (Osterbrock 1969; Mason 1975; Grandi 1978). In general, the line ratios (Table 5) are quite close to those expected from models in which the ions coexist in a collisionally ionized and excited gas near 10^6 K. For IIIZw77 (Osterbrock 1981), however, the ratio $I(\lambda 5303)/I(\lambda 6374)$ suggests a temperature 1.35×10^6 K, whereas that derived from $I(\lambda 6374)/I(\lambda 7892)$ is only 1.02×10^6 K, implying that a distribution of gas temperatures is needed in the collisional model. Existing photoionization models (Osterbrock 1969; Grandi 1978), which assume a point ionizing continuum source with flux proportional to $\nu^{-1.24}$, predict a much more rapid decline in line intensity with increasing degree of ionization than is generally observed (Table 5). It seems

Table 5. High ionization line ratios.

Lines	Observed ratio (comment)	Theoretical ratio (ref.)		
		Collisional		Photoionization
		$T \sim 10^6$	$T \sim 1.5 \times 10^6$	
$\frac{I_{6374}}{I_{7892}}$	1.9 (mean, see text)	2.22 (1)	0.46 (1)	11 (2)
$\frac{I_{5303}}{I_{6374}}$	$\lesssim 0.15$ (3) ~ 0.32 (4) ~ 0.05 (5)	0.002 (1)	1.1 (1)	0.11 (6)
$\frac{I_{2649}}{I_{7892}}$	2 (7) < 2.3 (5)	0.5 (8)	0.5 (8)	$0.9 \exp \frac{-35\,300}{T}$ (9)

1. Mason (1975).
2. Grandi (1978).
3. In Tol 0109 – 383.
4. In IIIZw77 (Osterbrock 1981).
5. In NGC 3783 (Ward & Morris 1984).
6. Osterbrock (1969).
7. In NGC 4151.
8. Mason (private communication, 1978).
9. Using the collision strengths and A-values of Mason (1975) and, taking account of excitation of $^3P_0$, $^3P_1$ and $^1D_2$, this formula is good to better than 5 per cent at temperatures above 5×10^3 K but low enough that cascades from higher states are unimportant.

likely that photoionization models (which are favoured by the correlations of [Fe X] and [Fe XI] with Hβ, [Fe VII] and [O III] line intensities) could give better fits to the intensity ratios of [Fe X], Fe XI] and [Fe XIV] if they invoked a flatter ionizing continuum. We are not aware of such models, which are needed to test whether the flatter spectrum can produce the necessary large changes in relative line intensities.

5.2 DENSITY

Unfortunately, there is no direct way of determining the electron density n_e (cm^{-3}) of the Fe^{9+} region. Probably the best approach is to relate the luminosity of the [Fe X] line to n_e, the volume, V (cm^3), and the filling factor, ϵ, of the clouds from which the line originates. If V can be estimated in some other way, limits on n_e and ϵ can be obtained.

In the collisional ionization picture, equation (10) of Nussbaumer & Osterbrock (1970) may be used to show

$$L_{40}[\text{Fe X}] = 7.1 \times 10^{-66} n_e^2 V\epsilon \qquad (1)$$

where $L_{40}([\text{Fe X}])$ is the luminosity of the λ6374 line in units of 10^{40} erg s^{-1}. In this equation, we have assumed $\log T_e = 6.1$ (at which temperature the rate of emission in the line is maximized) and $N(\text{Fe})/N(\text{H}) \simeq 10^{-5}$. In the case of photoionization, it is necessary to consider excitation of [Fe X] by both collisions and resonance fluorescence caused by the large ultraviolet photon flux (Osterbrock 1969). Following Osterbrock, we assume $N(Fe^{9+}) = N(\text{Fe})$ and $T_e = 2.5 \times 10^4$ K in the zone of interest and an ionizing continuum flux density of the form

$$F_\nu = \text{constant } (\nu/\nu_H)^{-1.24} (2 \times 10^7/D)^2 \text{ erg cm}^{-2} \text{ s}^{-1} \text{ Hz}^{-1}. \qquad (2)$$

Here $h\nu_H = 13.6$ eV and D is the distance from the point continuum source in pc. Equation (2) is consistent with the suggestion from ultraviolet observations of NGC 4151 (Penston *et al.* 1981), for which galaxy the constant in equation (2) = 6.0×10^{-26}. The contribution of collisional excitation to the emissivity in [Fe x] is given directly by Osterbrock's (1969) equation (5). In order to calculate the resonance fluorescence, whose emissivity is given by Osterbrock's (1969) equation (6), we have assumed that the inner, mean and outer radii of the Fe^{9+} zone each scale from galaxy to galaxy as $D \propto L^{1/2} n_e^{-1/2}$, where L is the ionizing luminosity and n_e is independent of distance. In other words, each of these radii is determined by a certain ionization parameter $L/n_e D^2$, whose value is taken from Osterbrock's (1969) calculation for the particular case of NGC 4151 with $n_e = 10^4\,\mathrm{cm}^{-3}$. Under these assumptions, along with the same spectral index, but different central source luminosity (*cf.* equation 2) and n_e from galaxy to galaxy, the total luminosity in [Fe x] in the photoionization model becomes.

$$L_{40}[\mathrm{Fe\ x}] = 1.0 \times 10^{-65} n_e^2 V\epsilon. \tag{3}$$

Note that the [Fe x] *emissivity* (i.e. energy radiated per unit volume) is, under our assumptions, independent of the constant in equation (2) because F_ν at the relevant frequencies of the fluorescence transitions is independent of L for a fixed value of n_e. Of course, V does depend on L. The n_e^2 dependence results from Osterbrock's equation (6) and our assumption of fixed ionization parameter in the Fe^{9+} zone, which imply $F_\nu \propto n_e$. As may be seen by comparing equations (1) and (3), the formulae for collisional and photoionization are very similar.

Limits on the density and size of the Fe^{9+} zone may be obtained in two ways. First, a lower limit to the size can be assigned by noting that the [Fe x] λ 6374 line is not formed at a density more than one or two orders of magnitude higher than the critical density of $1.2 \times 10^{10}\,\mathrm{cm}^{-3}$. To see this one may compare line strengths and emission measures of the iron line and Hβ. It is difficult to tell what proportion of the Hβ line actually comes from the Fe^{9+} region but the Hβ line strength from this region is certainly not greater than 10 times that of λ 6374. Using the emission measure of $1.25 \times 10^{-23} T^{-1/2}\,\mathrm{erg\,cm^{-2}\,s^{-1}}$ for Hβ (Osterbrock 1974) and equations (1) and (3) above, one finds

$$\begin{aligned} n_e &< 7 \times 10^{10}\,\mathrm{cm}^{-3} && \text{(photoionization)} \\ &\quad 6 \times 10^{11} && \text{(collisional).} \end{aligned}$$

So if the Fe^{9+} region takes the form of a sphere of radius D_s pc, then

$$\begin{aligned} D_s &> 4 \times 10^{-5} (L_{40}[\mathrm{Fe\ x}]/\epsilon)^{1/3}\,\mathrm{pc} && \text{(photoionization)} \\ &\quad 1 \times 10^{-5} (L_{40}[\mathrm{Fe\ x}]/\epsilon)^{1/3} && \text{(collisional).} \end{aligned} \tag{4}$$

Secondly, the probable variability of [Fe x] in NGC 4151 (Section 1) may be used to set an upper limit on the size and a lower limit on the density. If the diameter of the Fe^{9+} region in NGC 4151 is less than 1 pc and assuming spherical symmetry, one finds for that galaxy

$$n_e > 4 \times 10^4 \epsilon^{-1/2}\,\mathrm{cm}^{-3} \tag{5}$$

which is essentially independent of the mode of ionization.

In the photoionization case, the volume of the emission region is related to the continuum fluxes near the ionization potentials of Fe^{8+} and Fe^{9+}. To estimate these fluxes we

adopt equation (2) and assume the ionizing luminosity scales linearly with the Hβ luminosity* from galaxy to galaxy

$$F_\nu = 1.8 \times 10^{27} (\nu/\nu_H)^{-1.24} L_{40}(H\beta)\,(2 \times 10^7/D)^2 \text{ erg cm}^{-2}\text{ s}^{-1}\text{ Hz}^{-1} \quad (6)$$

Here L_{40} (Hβ) is the Hβ luminosity in units of 10^{40} erg s^{-1}. The inner and outer radii of the Fe^{9+} zone each then scale as the square root of the ionizing luminosity and, following Osterbrock (1969), the volume of the Fe^{9+} region is

$$V = 2 \times 10^{62} n_e^{-3/2} L_{40}(H\beta)^{3/2}\text{ cm}^3 \quad (7)$$

with an outer radius

$$D_0 = 120\, n_e^{-1/2} L_{40}(H\beta)^{1/2}\text{ pc}. \quad (8)$$

Combination of equation (3) with (7) yields a relation between n_e, ϵ, L_{40} [Fe x] and L_{40} (Hβ)

$$n_e \epsilon^2 = 3 \times 10^5 L_{40}(H\beta)^{-3} L_{40}[\text{Fe x}]^2\text{ cm}^{-3}. \quad (9)$$

Equation (9) is closely related to homology arguments, which predict the same line ratios from models in which $n_e \epsilon^2 L$ is the same (*cf.* Scargle, Caroff & Tarter 1974) and shows that the [Fe x] to Hβ luminosity should increase with increasing luminosity for the same conditions (i.e. n_e and ϵ) in the Fe^{9+} region. No such effect, indeed some evidence to the contrary, is found in the data. In consequence, the product $n_e \epsilon^2$ ranges from 6.6×10^2 cm^{-3} for Tol0109 – 383 to $< 10^{-3}$ cm^{-3} for MCG-2-58-22 in a way which is generally anticorrelated with luminosity. This effect suggests that n_e may decrease with D, which would serve to decrease the mean density in the more extensive Fe^{9+} regions of the more luminous galaxies. However, the results of this very simple model clearly need checking by full computer calculations of photoionization models of the highly ionized regions. If we adopt equation (9) for NGC 4151 and combine it with equation (5), which is based on the supposed variability of [Fe x] in that galaxy, one obtains

$$n_e \geqslant 2.2 \times 10^6\text{ cm}^{-3}$$
$$\epsilon \leqslant 3 \times 10^{-4}. \quad (10)$$

5.3 KINEMATICS

As noted in Section 3, the [Fe x] λ 6374 line tends to be both broader than lines of low-ionization species and blueshifted with respect to the systemic velocity. Similar effects have been found for other high-ionization lines – [O III] λ 5007 (Heckman *et al.* 1981; Mirabel & Wilson 1984; Section 3 of this paper) and [Fe XI] λ 7892 (Grandi 1978). There is a general consensus that these lineshifts should be accounted for in terms of radial motions in an absorbing medium, although both inflow and outflow pictures are compatible with the data.

In the inflow case, the blueshift can be produced if the individual filaments of the high-ionization regions have internal absorption. Then those on the far side of the object emit in the direction of the Earth unabsorbed whereas the line emission from this side of the nebula reaches us through the back of the absorbing filament. Such a model assumes photoionization for the Fe^{9+} and Fe^{10+} regions to provide the high-ionization region on the inside of each

* This assumption is adopted because of the greater availability of Hβ than Lα data but, as noted, the fluctuations in the Lα-to-Hβ ratio are much less than the range in luminosity.

filament. An alternative inflow model would involve scattering of the line photons off 'moving mirrors', such as infalling electrons or dust particles. Scattering off dust would again require accompanying absorption and substantially higher emitted flux.

An outflow model would envisage the line emitting filaments to be immersed in a dust filled medium (*cf.* Heckman *et al.* 1981) or the presence of an opaque central object, for example, an accretion disc. Filaments on the far side of the nucleus would then be preferentially attenuated compared to those on the near side. Both inflow and outflow models predict that the blueshift effect should be more marked for bluer lines. No comparison is possible with the present data, the velocities of [Fe X] λ 6374 and [Fe XI] λ 7892 agreeing within their errors, but an interesting test may be possible if [Fe XI] λ 2649 can be observed at high enough dispersion with the *Space Telescope*.

In the long term, it may be possible to distinguish inflow from outflow by monitoring the response of the [Fe X] and [Fe XI] line profiles to a change in ionizing continuum, given that the Fe^{9+} and Fe^{10+} zones are within a few pc of the central source in the photoionization models. The effects of a change in the ionizing continuum on the [Fe X] and [Fe XI] emission lines will be noticed first for clouds on the near side of the nucleus. For an inflow model and, say, an increase in the ionizing continuum, the red wing of the line should increase first; on the other hand, if outflow is the correct picture the blue side of the line will initially be enhanced.

6 Conclusions

Our discussion of [Fe X] λ 6374 (and other lines of highly ionized species) in Seyfert galaxies has focused on the ionization mechanism and kinematics of the Fe^{9+} region. The good correlation of the intensities of [Fe X] λ 6374 and [Fe XI] λ 7892 with those of [Fe VII] λ 6087 and [O III] λ 5007, both of which are known to arise from gas at $T_e \simeq (1-3)\times 10^4$ K, supports photoionization as the mode of energy input for all these species. The probable trend relating [Fe X] λ 6374 and Hβ intensities is also consistent with a photoionization picture. On the other hand, the lack of correlation with the soft X-ray intensities only a decade away in wavelength from the ionization potential of Fe^{8+} is puzzling. Also, current photoionization models do not reproduce well the relative intensities of the [Fe X], [Fe XI] and [Fe XIV]lines, although the discrepancy is in part a consequence of the oversimplified approach and the unrealistic assumptions used in the models. These line ratios can be modelled by collisional ionization in a gas with a range of temperatures between 1.0×10^6 and 1.5×10^6 K. Independent of the mode of ionization, the radius of the Fe^{9+} zone in NGC 4151 lies between 1×10^{-4} and 0.5 pc and its density between 4×10^4 and 6×10^{11} cm^{-3}. These limits are derived from the absence of strong collisional de-excitation and the probable variability of [Fe X] λ 6374 in this galaxy.

With regard to the kinematics of the gas, [Fe X] λ 6374, [Fe XI] λ 7892 and [O III] λ 5007 tend to be blueshifted with respect to the systemic velocity (as defined by H I λ 21 cm emission or optical lines of low ionization species like [O I] λ 6300) and are also broader than [O I] λ 6300. These blueshifts almost certainly reflect radial motions in a dust filled medium, although both inflow and outflow models are consistent with the data. The broad lines of [Fe X] and [Fe XI], the small radii of the Fe^{9+} and Fe^{10+} zones and their high densities (see above) support the concept (Wilson 1979; Pelat, Alloin & Fosbury 1981) that these lines originate from a region between the conventional broad and narrow line regions. In this connection, it is interesting to note that [Fe X] λ 6374 is seen as often in our sample of type 2 Seyfert galaxies as in those of type 1, suggesting small high density regions may exist in the former galaxies.

Future work would be useful in a number of areas. First, realistic photoionization models for [Fe X] and [Fe XI], including ranges of spectral shapes for the ionizing continuum and of variations of gas density with distance from the centre would be valuable. Secondly, a search for variability of [Fe X] λ6374 and [Fe XI] λ7892 could constrain the scale and density of the high ionization zones in more objects. Lastly, measurement of the strength of [Fe XI] λ2649 might, when combined with simultaneous data on [Fe XI] λ7892, allow a temperature measurement of sufficient accuracy to distinguish photo- from collisional ionization. The profile of this UV line is also of interest for the kinematics of the Fe^{10+} region, but must await the *Space Telescope*.

Acknowledgments

We thank the relevant allocation committees for time on the AAT and 200-in telescopes. One author (ASW) thanks another (AB) for warm hospitality during a visit to the Royal Greenwich Observatory during the summer of 1982, when some of this work was performed. Dr J. P. Harrington provided valuable insight on photoionization models. MVP and RAEF acknowledge that many of their contributions to this work took place while they were at the Anglo-Australian Observatory and staff and visitor respectively at the ESA Villafranca Satellite Tracking Station.

References

Adams, T. F. & Weedman, D. W., 1975. *Astrophys. J.*, **199**, 19.
Anderson, K., 1970. *Astrophys. J.*, **162**, 743.
Barr, P., Pollard, G., Sanford, P. W., Ives, J. C., Ward, M. J., Hine, R. G., Longair, M. S., Penston, M. V., Boksenberg, A. & Lloyd, C., 1980. *Mon. Not. R. astr. Soc.*, **193**, 549.
Boksenberg, A. & Netzer, H., 1977. *Astrophys. J.*, **212**, 37.
Boksenberg, A., Shortridge, K., Allen, D. A., Fosbury, R. A. E., Penston, M. V. & Savage, A., 1975. *Mon. Not. R. astr. Soc.*, **173**, 381.
Cooke, B. A., Elvis, M., Maccacaro, T., Ward, M. J., Fosbury, R. A. E. & Penston, M. V., 1976. *Mon. Not. R. astr. Soc.*, **177**, 121P.
Elvis, M. S., Maccacaro, T., Wilson, A. S., Ward, M. J., Penston, M. V., Fosbury, R. A. E. & Perola, C. G., 1978. *Mon. Not. R. astr. Soc.*, **183**, 129.
Feldman, F. R., Weedman, D. W., Balzano, V. A. & Ramsey, L. W., 1982. *Astrophys. J.*, **256**, 427.
Fosbury, R. A. E., Mebold, U., Goss, W. M. & Dopita, M. A., 1978. *Mon. Not. R. astr. Soc.*, **183**, 549.
Fosbury, R. A. E. & Sansom, A. E., 1983. *Mon. Not. R. astr. Soc.*, **204**, 1231.
Grandi, S. A., 1978. *Astrophys. J.*, **221**, 501.
Heckman, T. M., Balick, B. & Sullivan, W. T., 1978. *Astrophys. J.*, **224**, 745.
Heckman, T. M., Miley, G. K., Van Breugel, W. J. M. & Butcher, H. R., 1981. *Astrophys. J.*, **247**, 403.
Jefferies, J. T., 1969. *Mem. Soc. R. Sci. Liège*, **17**, 213.
Koski, A. T., 1978. *Astrophys. J.*, **223**, 56.
Kriss, G. A., Canizares, C. R. & Ricker, G. R., 1980. *Astrophys. J.*, **242**, 492.
Mason, H., 1975. *Mon. Not. R. astr. Soc.*, **170**, 651.
McHardy, I. M., Lawrence, A., Pye, J. P. & Pounds, K. A., 1981. *Mon. Not. R. astr. Soc.*, **197**, 893.
Mirabel, I. F. & Wilson, A. S., 1984. *Astrophys. J.*, in press.
Netzer, H., 1974. *Mon. Not. R. astr. Soc.*, **169**, 579.
Neugebauer, G., Becklin, E. E., Oke, J. B. & Searle, L., 1976. *Astrophys. J.*, **205**, 29.
Nussbaumer, H. & Osterbrock, D. E., 1970. *Astrophys. J.*, **161**, 811.
Oke, J. B. & Sargent, W. L. W., 1968. *Astrophys. J.*, **151**, 807.
Osmer, P. S., Smith, M. G. & Weedman, D. W., 1974. *Astrophys. J.*, **189**, 187.
Osterbrock, D. E., 1969. *Astrophys. Letts.*, **4**, 57.
Osterbrock, D. E., 1977. *Astrophys. J.*, **215**, 733.
Osterbrock, D. E., 1981. *Astrophys. J.*, **246**, 696.
Osterbrock, D. E. & Koski, A. T., 1976. *Mon. Not. R. astr. Soc.*, **176**, 61P.

Pelat, D., Alloin, D. & Fosbury, R. A. E., 1981. *Mon. Not. R. astr. Soc.*, **195,** 787.
Penston, M. V. & Fosbury, R. A. E., 1978. *Mon. Not. R. astr. Soc.*, **183,** 479.
Penston, M. V., Boksenberg, A., Bromage, G. E., Clavel, J., Elvius, A., Gondhalekar, P. M., Jordan, C., Lind, J., Lindegren, L., Perola, G. C., Pettini, M., Snijders, M. A. J., Tanzi, E. G., Tarenghi, M. & Ulrich, M. H., 1981. *Mon. Not. R. astr. Soc.*, **196,** 857.
Phillips, M. M. & Osterbrock, D. E., 1975. *Publ. astr. Soc. Pacific.*, **87,** 949.
Piccinotti, G., Mushotzky, R. F., Boldt, E. A., Holt, S. S., Marshall, F. E., Serlemitsos, P. J. & Shafer, R. A., 1982. *Astrophys. J.*, **253,** 485.
Scargle, J. D., Caroff, L. J. & Tarter, C. B., 1974. *Astrophys. J.*, **189,** 181.
Schmidt, G. D. & Miller, J. S., 1980. *Astrophys. J.*, **240,** 759.
Shields, G. A., 1974. *Astrophys. J.*, **191,** 309.
Tyagun, N. F., 1977. *Pis'ma v Astron. Zh.*, **3,** 559. (*Sov. astr. Letts.*, **3,** 305.)
Ward, M. J., 1978. Unpublished. *D Phil thesis*, University of Sussex.
Ward, J. J., Wilson, A. S., Penston, M. V., Elvis, M., Maccacaro, T. & Tritton, K., 1978. *Astrophys. J.*, **223,** 788.
Ward, M. J. & Morris, S., 1984. *Mon. Not. R. astr. Soc.*, in press.
Weedman, D. W., 1971. *Astrophys. J.*, **167,** L23.
Weedman, D. W., 1976. *Astrophys. J.*, **208,** 30.
West, R. M., Borchkhadze, T. M., Breysacher, J., Lautsen, S. & Schuster, H. E., 1978. *Astr. Astrophys. Suppl.*, **31,** 55.
Wilson, A. S., 1979. *Proc. R. Soc. London*, **A366,** 461.
Wilson, A. S. & Penston, M. V., 1979. *Astrophys. J.*, **232,** 389.
Wilson, A. S., Penston, M. V., Fosbury, R. A. E. & Boksenberg, A., 1976. *Mon. Not. R. astr. Soc.*, **177** 673.
Yee, H. K. C., 1980. *Astrophys. J.*, **241,** 894.